$K^{\pm}$ P ELASTIC SCATTERING AT 180 DEGREES FROM 0.40 TO 0.73 GEV/C

by

Paul Kendall Caldwell

A Dissertation Submitted to the Faculty of the

DEPARTMENT OF PHYSICS

In Partial Fulfillment of the Requirements
For the Degree of

DOCTOR OF PHILOSOPHY

In the Graduate College

THE UNIVERSITY OF ARIZONA

1969

THE UNIVERSITY OF ARIZONA

GRADUATE COLLEGE

I hereby recommend that this dissertation prepared under my direction by Paul Kendall Caldwell

entitled $K^{\pm}$ P Elastic Scattering at 180 Degrees From 0.40 to 0.73 Gev/c

be accepted as fulfilling the dissertation requirement of the degree of Ph.D.

Elmer W. Jenkins — Dissertation Director

8/11/69 — Date

After inspection of the final copy of the dissertation, the following members of the Final Examination Committee concur in its approval and recommend its acceptance:*

John A. Stoner, Jr.	11 August 1969
John R. Leavitt	11 August 1969
Theodore Bowen	11 August 1969
William J. Baikal	Aug 11/69

*This approval and acceptance is contingent on the candidate's adequate performance and defense of this dissertation at the final oral examination. The inclusion of this sheet bound into the library copy of the dissertation is evidence of satisfactory performance at the final examination.

STATEMENT BY AUTHOR

This dissertation has been submitted in partial fulfillment of requirements for an advanced degree at The University of Arizona and is deposited in the University Library to be made available to borrowers under rules of the Library.

Brief quotations from this dissertation are allowable without special permission, provided that accurate acknowledgment of source is made. Requests for permission for extended quotation from or reproduction of this manuscript in whole or in part may be granted by the head of the major department or the Dean of the Graduate College when in his judgment the proposed use of the material is in the interests of scholarship. In all other instances, however, permission must be obtained from the author.

SIGNED: Paul Caldwell

ACKNOWLEDGEMENTS

This dissertation represents the combined efforts of all those who helped in the design, construction, operation, and analysis of the $K^{\pm}$ p scattering experiments done by the University of Arizona between December, 1968 and June, 1969.

I am particularly grateful to Dr. E. W. Jenkins, who directed the experiments and guided this dissertation, and to Dr. T. Bowen and Dr. R. M. Kalbach for all their assistance and helpful discussions. My thanks also go to Dr. A. E. Pifer, who helped analyze the data, and assisted in all other phases of the experiments along with Dr. F. N. Dikmen and D. V. Petersen. Further assistance in the construction was provided by our machinist, W. K. Black, our electronics technician, C. L. Sullivan, and by W. T. Beauchamp and R. E. Rothschild. Assisting in the operation were D. Davidson, J. Davidson, E. P. Krider and J. A. Zika.

We are all indebted to the staff of Lawrence Radiation Laboratory, Berkeley, California, for their help in carrying out these experiments. Particular thanks are due the operators and crew of the Bevatron.

Lastly, I wish to thank my wife, Audrey, for her encouragement and understanding, and also for correcting and typing this manuscript.

TABLE OF CONTENTS

LIST OF ILLUSTRATIONS

LIST OF TABLES

ABSTRACT

The $K^{\pm}$ p elastic scattering was measured in a small angular region near 180° ($-.995 \geq \cos\theta_{c.m.} \geq -1$) at momenta ranging from 0.4 to 0.73 Gev/c. The experiment detected the forward-scattered protons with scintillation counters.

The K^{+} p data are used to compute the p-wave contributions to the scattering assuming s-wave dominance. The p-wave phase shift $(2\delta_{1+} + \delta_{1-})$ is found to be negative in the region 0.40 to 0.55 Gev/c. The K^{-} p elastic differential cross-section is found to dip smoothly to a minimum (0± 0.2 mb/steradian) at 0.66 Gev/c.

INTRODUCTION

$\bar{K}N$ scattering below an incident laboratory momentum of 1.5 Gev/c is largely dominated by resonances. The most recent edition of the Review of Particle Properties (Barash-Schmidt et al 1969) lists 27 such resonant states. The study of their properties represents a major part of the study of the $\bar{K}N$ system. Conversely, the KN system exhibits no strong resonant behavior. Recently, very small effects which may be due to resonances have been reported in K^+ p scattering (Abrams et al 1967, Carroll et al 1968), but there is certainly no evidence that these dominate the scattering.

One of the more useful techniques for studying meson-nucleon scattering is the measurement of the differential cross-section at 180° (Kormanyos et al 1966, Derrick 1968). This is because at 180° the even and odd partial waves have opposite signs, and the constructive or destructive interference is maximized. In a region where a resonance occurs, measurement of the backward scattering may not only divulge its presence, but also determine the parity (Heinz and Ross 1965).

Backward scattering experiments at higher energies have been done by Banaigs et al (1967), Aderholz et al (1967), Ficenec and Trower (1967), and Carroll et al (1968). Carroll et al reported a possible K^+ p resonance at 1.46 Gev/c. Above 3.5 Gev/c the K^- p cross-section is less than 0.5 μbarns/steradian, while the K^+ p cross-section seems to be about 10 μbarns/steradian.

In the region of laboratory momenta below 0.75 Gev/c, the angular distributions of the K^+ p scattering have been measured by Goldhaber et al (1962), Stubbs et al (1961), and Kycia, Kerth, and Baender (1960). These experiments measured the entire angular distribution in twelve steps or less, and did not emphasize the region near 180°. In the K^- p system, elastic scattering data has been published recently by 1) Watson, Ferro-Luzzi, and Tripp (1963), 2) Holley et al (1967), and 3) Bertanza et al (1969). These data do not include momenta between 0.48 and 0.66 Gev/c. Both 2) and 3) omit the region near 180° from the angular distribution.

An opportunity to study $K^\pm$ p elastic scattering at 180° from 0.4 to 0.73 Gev/c was presented because this experiment proved highly compatible with a measurement of the $K^\pm$ p total cross-section in this momentum range carried out by the University of Arizona Physics Department from December, 1968 until June, 1969. These experiments were done concurrently at the Lawrence Radiation Laboratory Bevatron, Berkeley, California. Their purpose was to look for the presence or absence of structure in the $K^\pm$ p scattering.

METHOD AND APPARATUS

In the momentum range 0.40 to 0.73 Gev/c, the recoil kaon from an elastic scatter near 180° has a range in liquid hydrogen of less than ten centimeters. At 0.40 Gev/c, the range is less than two centimeters. Therefore, since a target length of about forty-five centimeters was chosen to obtain a reasonable counting rate, the elastic differential cross-section at 180° was measured entirely by detecting the forward-going protons. These were separated from residual beam particles principally by time-of-flight measurements, and also by their greater energy loss (dE/dx) on passing through scintillator.

Beam

The layout of the Bevatron low momentum $K^{\pm}$ beam is depicted in Figure 1. The kaon beam was produced by protons in the external proton beam striking a copper target 2 inches long by 3/32 inches vertically by 3/8 inches horizontally. Secondary particles produced at 5° were deflected into parallel trajectories by the first quadrupole doublet. After traversing the electrostatic separator, the particles were brought to a first focus at the position of the mass and momentum selecting slits inside the 8 inch quadrupole singlet. The last quadrupole doublet gave a second focus some 115 inches beyond their final aperture. The momentum of the beam was determined by the pair of 16 x 36 "C" magnets, M2 and M3, and by the 13 x 24 "C" magnet, M1. The momentum distribution,

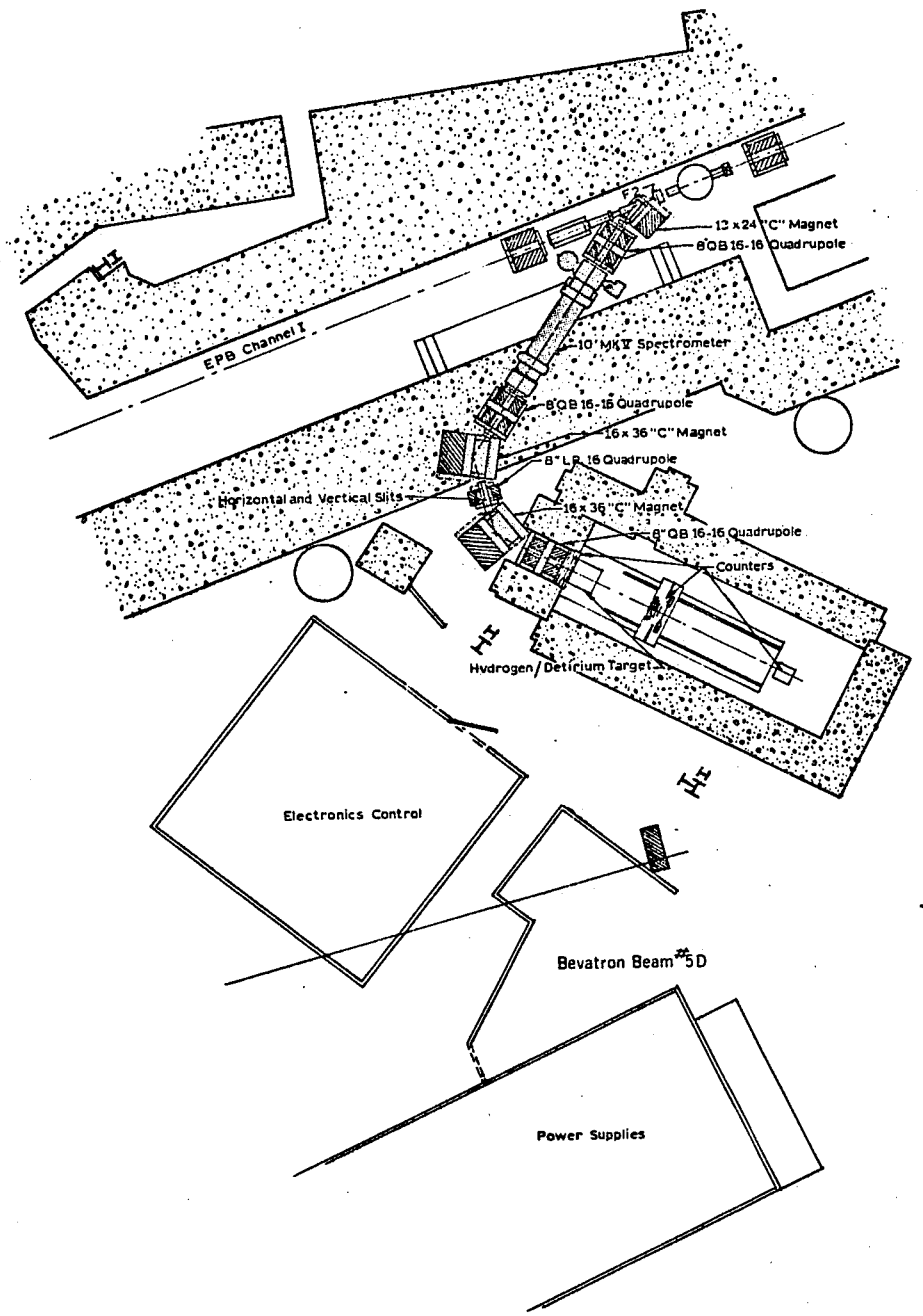

Figure 1. Layout of low momentum kaon beam.

generated by a computer program (TRACTUS) using the known magnet parameters, is shown in Figure 2.

The magnet currents were precalculated for each momentum at which data were taken. The field integrals were considered to be known functions of the currents (Bevatron Experimenter's Handbook 1969). Some additional tuning was required by the quadrupoles and the 13" x 24" "C" magnet M1. The tuning process maximized two quantities; the total number of kaons in the beam, and the total number of kaons which passed through a 5" diameter counter at the second focus. After the magnets were tuned, the momentum was checked by range measurements. The central momenta were found to be about 3/4 % lower than calculated, and are known to within 1/2 %.

Mass selection was provided by a ten foot electrostatic spectrometer with a four inch gap maintained at 600 kilovolts. The K-π vertical separation at 0.50 Gev/c was 0.7" (Bevatron Experimenter's Handbook 1969). The ratio of π's to K's was strongly momentum dependent, and is shown in Figure 3. The particle flux as a function of spectrometer magnet current is shown in Figure 4.

The total kaon flux as a function of momentum is shown in Figure 5.

Counters

The counters are shown schematically in Figure 6. S1 and C0 were located at the mass slit within the 8 inch quadrupole singlet. S2, C1, S3, and G were located after the last quadrupole doublet, and

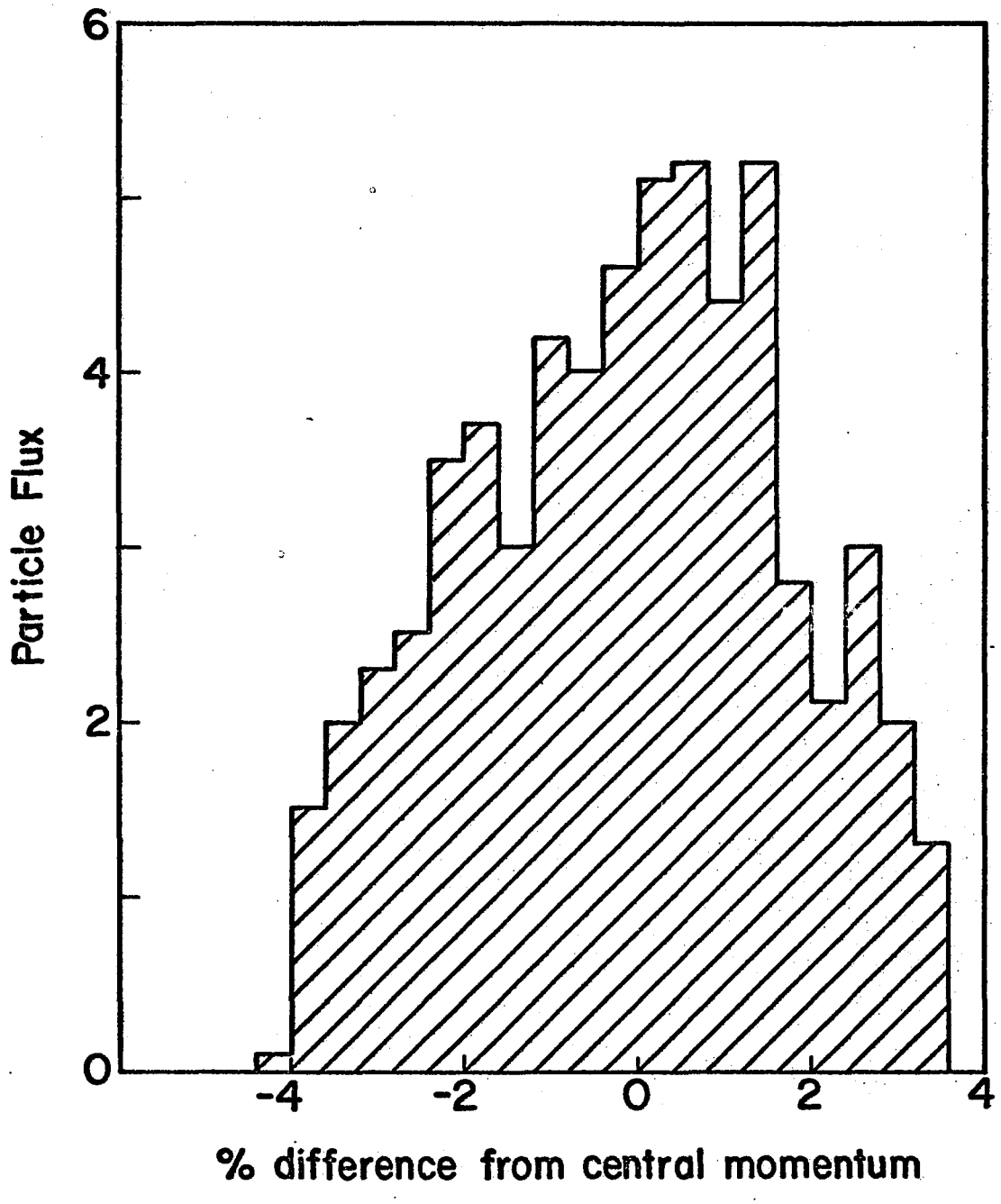

Figure 2. Momentum distribution of kaon beam.

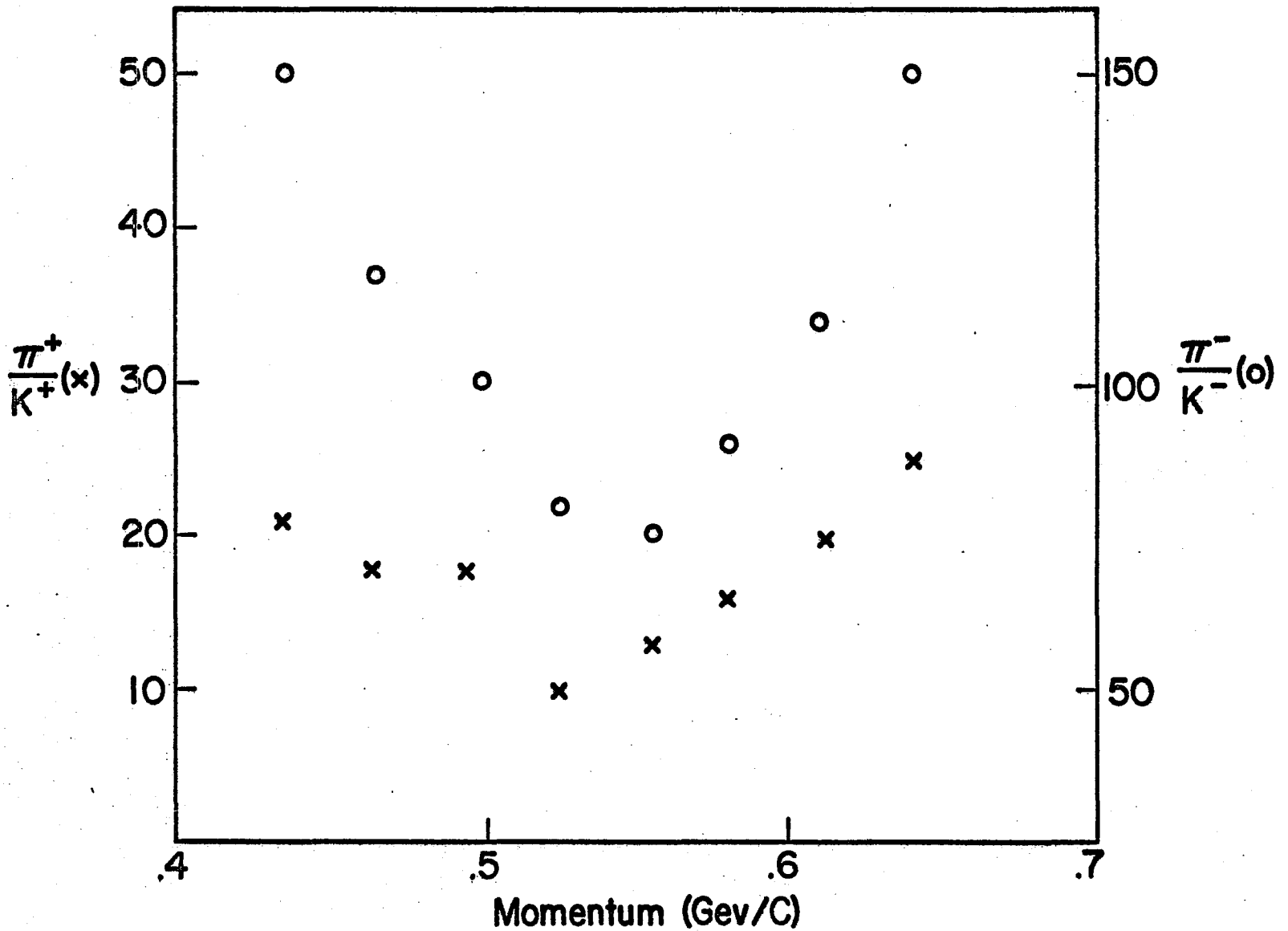

Figure 3. π/K vs. momentum.

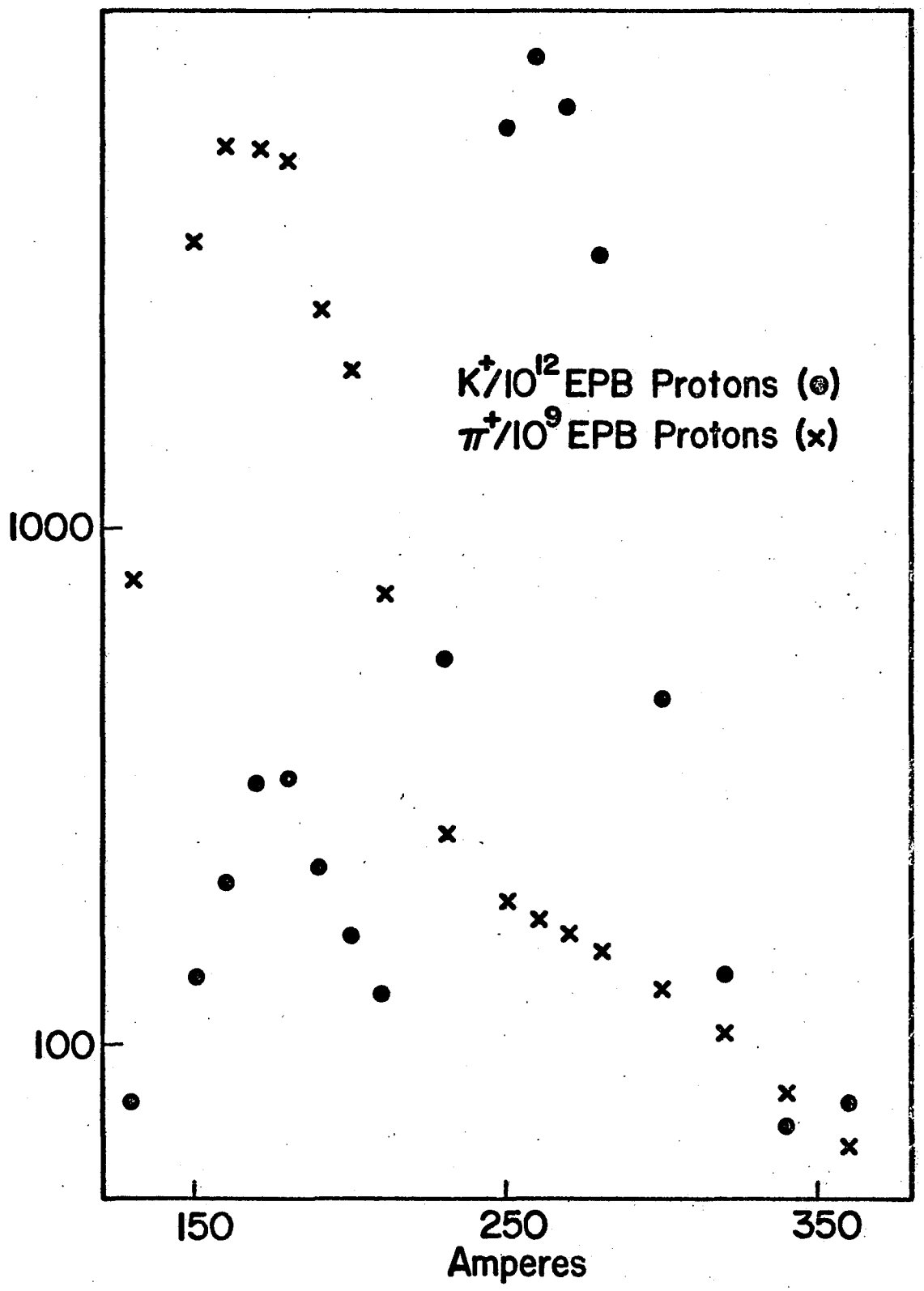

Figure 4. Typical particle flux vs. separator current.

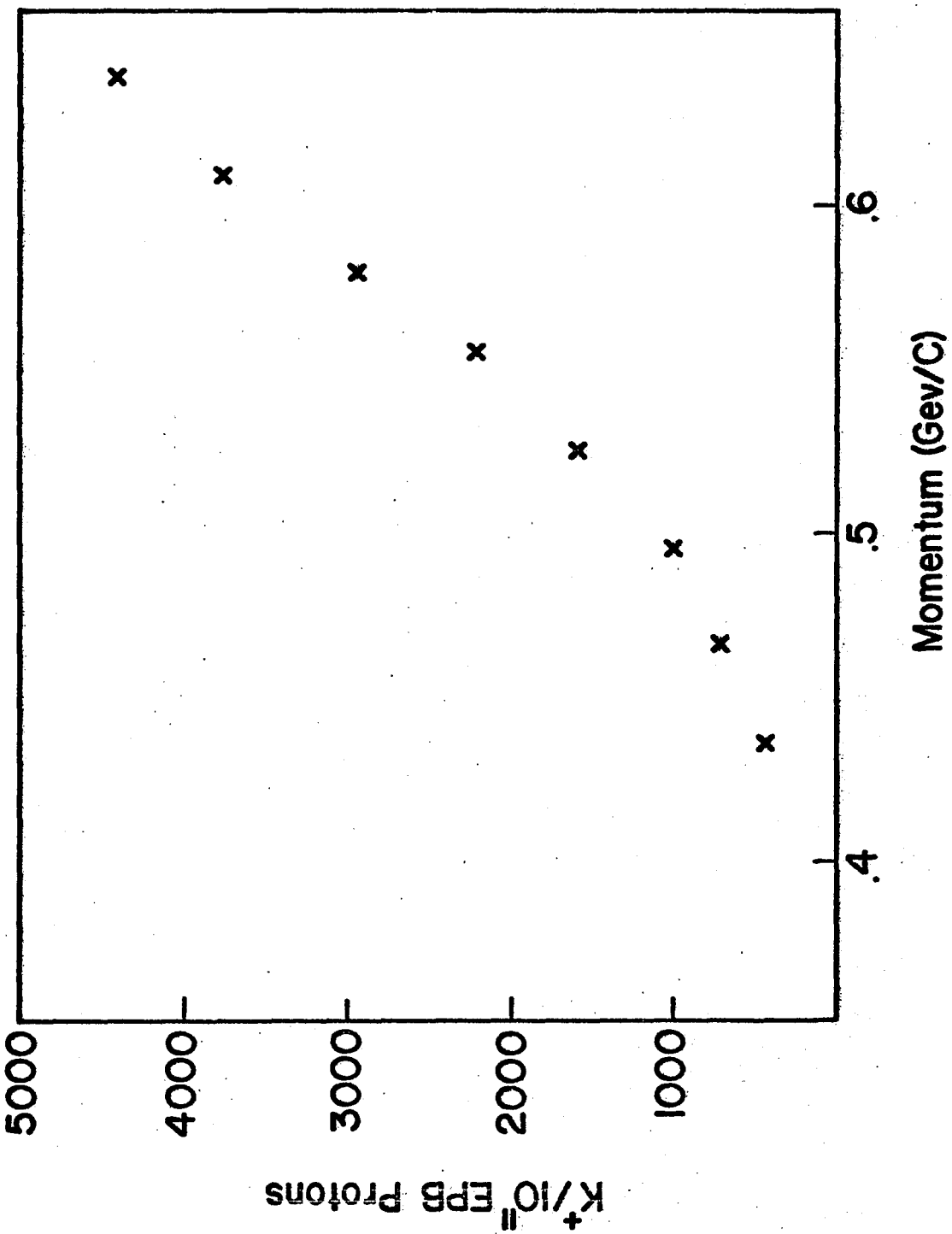

Figure 5. K^+ flux with Bevatron operating at I-27.

placed as close to the exit aperture as possible. All incoming beam particles were identified by signals from scintillation counters S1, S2, and S3. The components of these counters were chosen to minimize timing variations (Table I). Protons in the K^+ beam were rejected by dE/dx measurements in S1 and S3. This also rejected pairs of particles close enough together to cause large single pulses (doubles). The guard counter G vetoed off-line particles.

Particles less massive than kaons also produced signals in the Cherenkov counters C0 and C1. These counters were designed to operate in slightly different ways. C1 was a flat piece of lucite mounted perpendicularly to the beam so that only pion, muon, and electron light (totally reflected internally) would be collected by the photomultiplier tubes. In the momentum range 0.40 to 1.0 Gev/c, pions produce Cherenkov light which will be collected; kaons produce light which is largely lost through the front and back faces of the lucite. C0, on the other hand, was tilted at an angle of 40° to the beam. This angle was chosen so that Cherenkov light from the pions would go straight into the photomultiplier tube without reflections at 0.5 Gev/c. The downstream face of the counter was painted black, and the kaon light was absorbed on this surface. Although C0 was designed to operate only at 0.5 Gev/c, it performed equally well in the entire range of momenta at which data were taken because the velocity of the pions varied only ± 2 % from its value at 0.5 Gev/c.

Forward protons were identified by S4, S5, and C2. S4 and S5 were designed to minimize error in time-of-flight information (Table I).

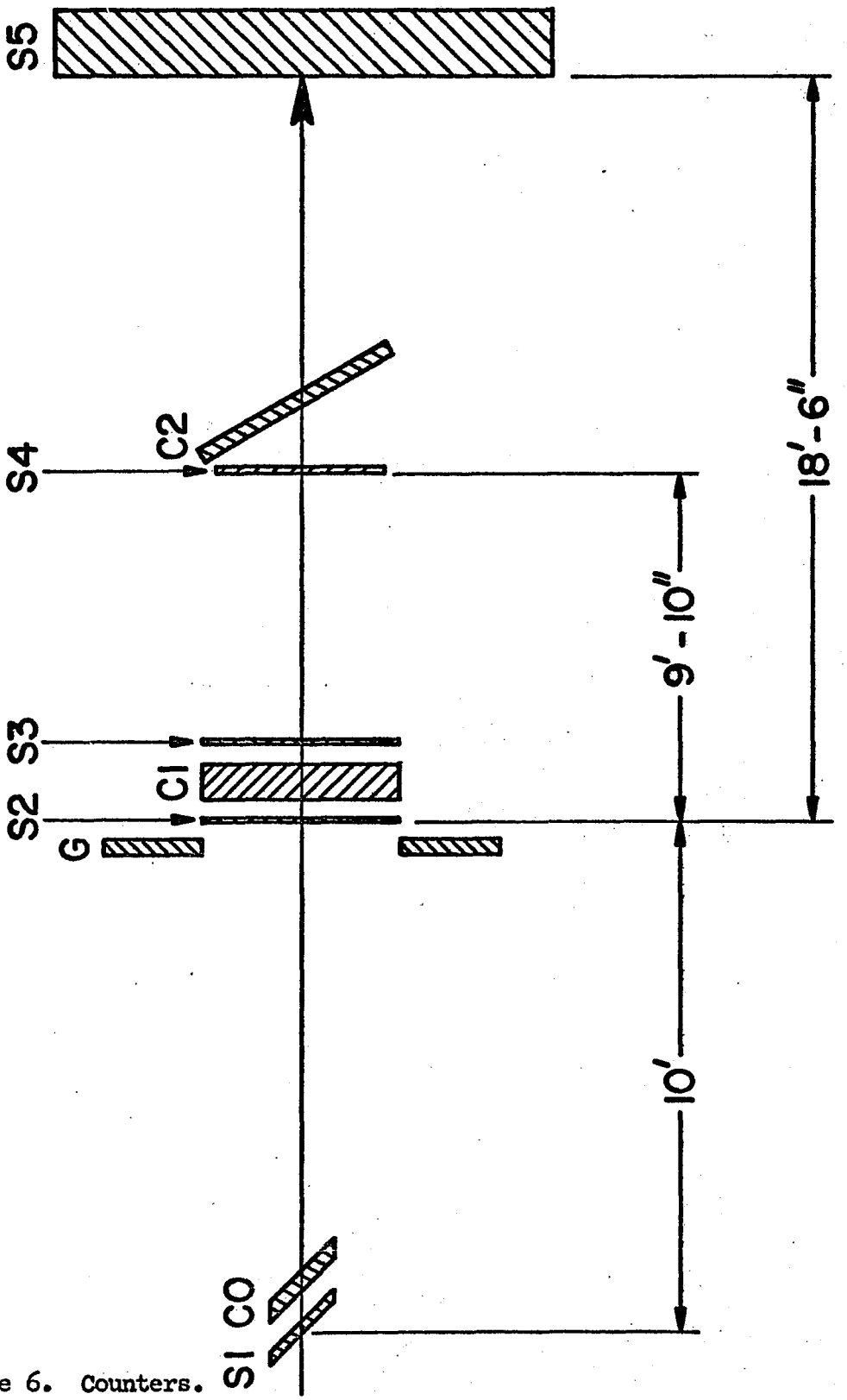

Figure 6. Counters.

Table I

COUNTERS

Counter	Type	Size	Material	Photomultiplier Tube(s)
S1	scintillation	5"x7/8"x1/8"	Pilot B	Amperex XP1021
C0	Cherenkov	12 3/4"x7/8"x1/2"	Lucite	RCA 8575
G	scintillation	10"dia. x 1/2" 3" x 6" cutout in center	NE 102	2-RCA 7746
S2	scintillation	3" x 6" x 1/8"	Pilot B	Amperex XP1021
C1	Cherenkov	3" x 6" x 1"	Lucite	2-RCA 8575
S3	scintillation	6"dia. x 1/8"	Pilot B	RCA 8575
S4	scintillation	5"dia. x 1/8"	Pilot B	Amperex XP1021
C2	Cherenkov	10" x 6" x 1/2"	Lucite	RCA 8522
S5	scintillation	15" dia. x 2"	Pilot F	Amperex XP1040

The scintillation counter S4 was 5 inches in diameter and defined the solid angle within which events were accepted. S5 was 15 inches in diameter. This counter provided time-of-flight information in order to separate events from beam particles, and consequently, the photomultiplier tube was mounted directly behind the scintillator to minimize variations in transit time. Since no plastic light guide was used, the scintillator was made two inches thick to provide enough signal to make the time information reliable. This arrangement reduced timing variations due to the geometry of S5 to .25 nanoseconds. S4 and S5 were also used to reject beam particles by dE/dx measurements, since the kaon pulse height was typically .75 or less that of an event pulse height.

C2 was a lucite Cherenkov counter mounted at 60° to the beam line except at 0.721 Gev/c, when it was mounted at 75° to the beam line. This counter rejected any remaining pion, muon, or electron contamination, and rejected some kaons at momenta above 0.5 Gev/c (Figure 7). Light from the faster particles was reflected internally into the photomultiplier tube, while any light generated by the events was lost through the downstream face of the counter.

Target

The hydorgen target was a mylar flask 18 inches long by 6 inches in diameter, and was supplied continuously with liquid hydrogen from a reservoir directly above the target vessel. Since the reservoir was open to the air, the density of the liquid hydrogen is taken to be 0.0706 ±0.0003 grams/cubic centimeter.

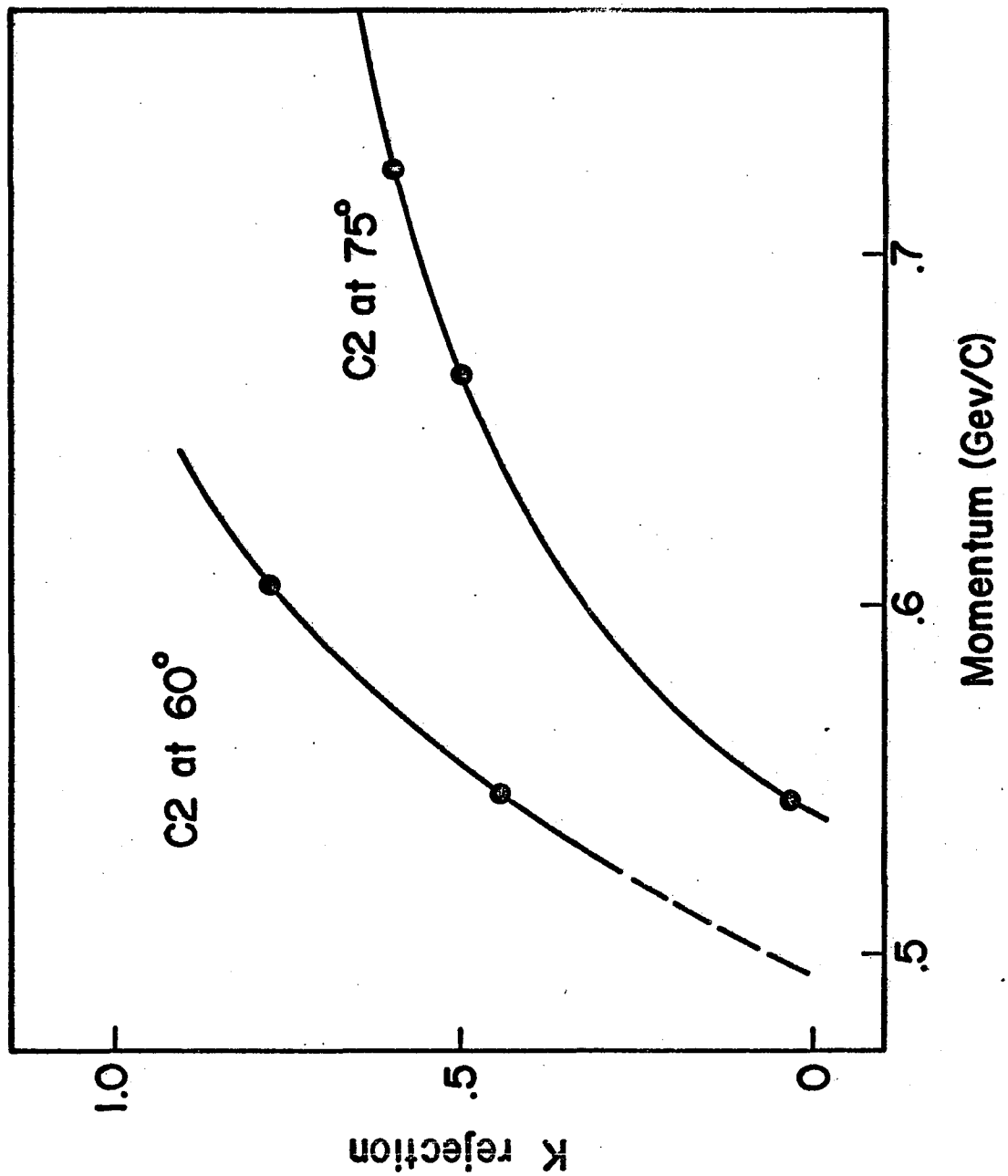

Figure 7. K rejection by C2 vs. incident beam momentum.

The target length was chosen to be 18 inches to provide a sufficient counting rate, but not be so long as to stop protons from 180° elastic scatters in the extreme upstream end of the target. It was also desired to keep the momentum loss of the kaons in the target at a mimimum. Kaons which enter the target at 0.428 Gev/c exit at about 0.392 Gev/c. This spread diminishes as the momentum increases, and is less than 20 Mev/c at the incident momentum of 0.735 Gev/c. The effective length of the target is determined by weighting the physical dimensions of the flask by the beam distribution measured at the target exit, Figure 8, and is found to be 44.6 centimeters.

In addition to the hydrogen flask there was a dummy flask, identical in every respect except content. Background measurements consisted of running exactly as during data taking periods, except with the empty flask.

Electronics

Kaon Identification

Figure 9 is a schematic diagram of the electronics which identified the incident kaons. All scintillation counters except G are connected to both a high level discriminator (called "slow") and a low level discriminator (called "fast"), which provided noise rejection along with good leading edge timing. S1 and S3 each had a third discriminator to provide the dE/dx information used to reject protons and doubles.

An output pulse from $\overline{G}S1S2S3$ denoted a beam particle unaccompanied by any off-line particle which would cause a signal in $\overline{G}$.

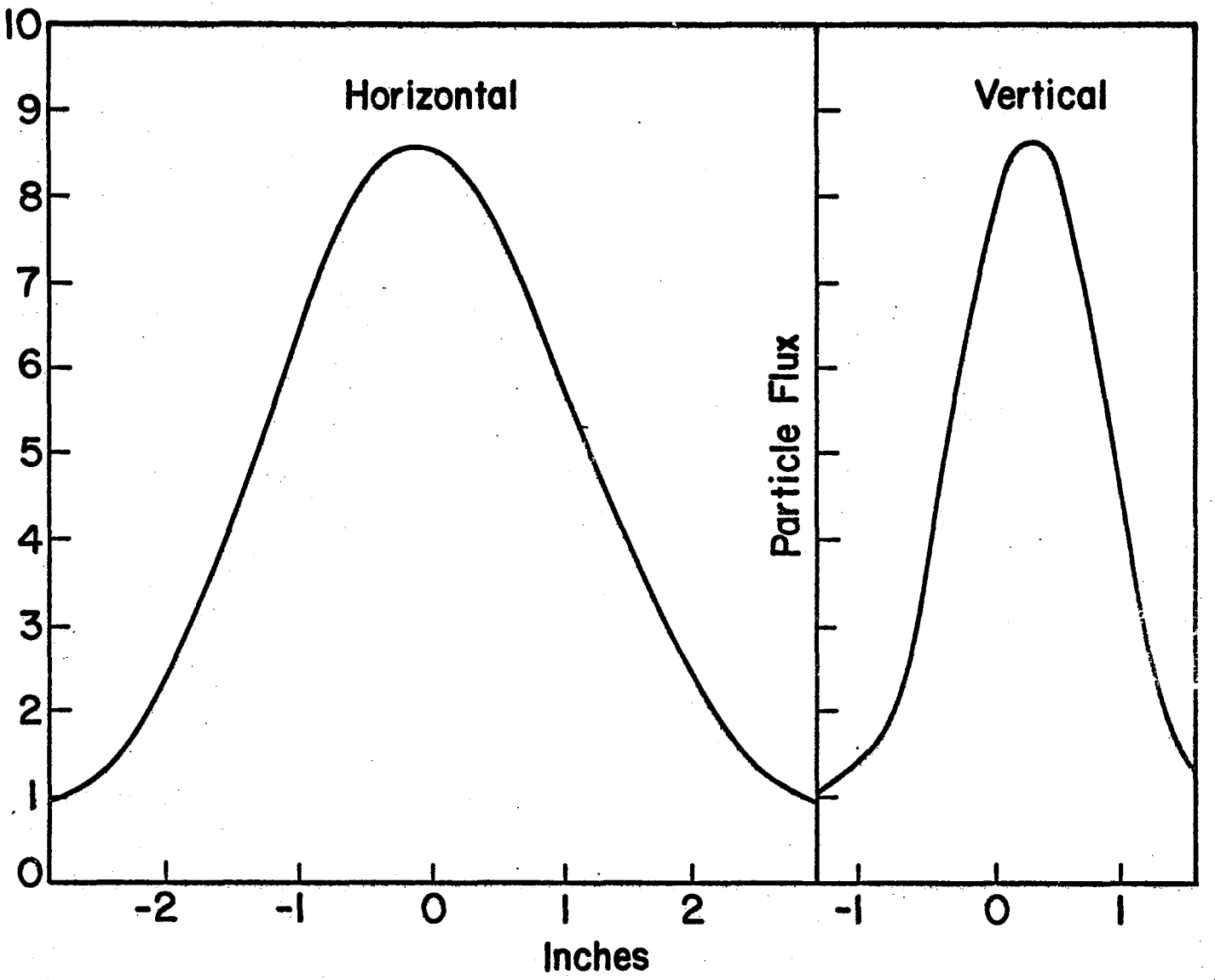

Figure 8. Spatial distribution of the beam.

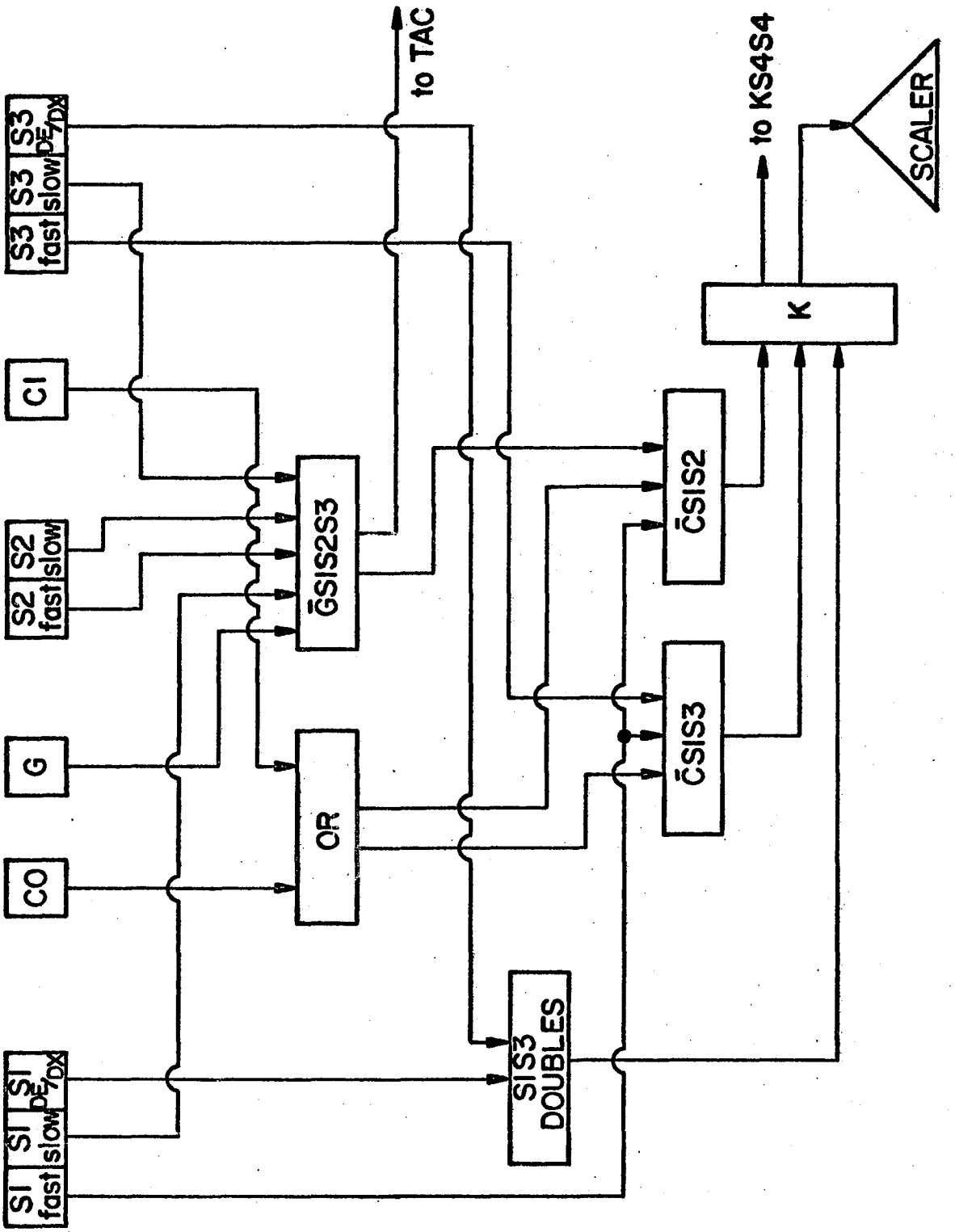

Figure 9. Incident beam telescope electronics.

Pile-up due to bunching of the beam particles was eliminated at this point by operating S3 slow in a mode that included 50 nanoseconds of dead time after each pulse. This discriminator was of the updating variety, and its output pulse was set for 60 nanoseconds duration. It was clipped after 10 nanoseconds as depicted in Figure 10. Sixty nanoseconds was considered adequate time for the 25 Megacycle scalers to record each event. Because of this feature, a second beam particle within 50 nanoseconds of the first will be ignored by the electronics. No dead time or accidental corrections to the data are necessary.

The output of $\overline{C}S1S2S3$ was initiated by S2 fast, and consequently preserved the time information from S2. Regenerating the S2 fast signal in this manner gives a signal that is undiluted with noise. To do this it is necessary to have the discriminator output pulses arrive at the logic unit inputs in the manner shown in Figure 11.

$\overline{C}S1S2$ and $\overline{C}S1S3$ are coincidences between fast discriminator outputs, and identify kaons by time-of-flight. The $\overline{C}$ anticoincidence signals from the Cherenkov counters C0 and C1 are also brought in at this point. These outputs, along with the S1S3 doubles in anticoincidence, go into the final logic circuit, K. An output signal from this unit denotes the passage of a kaon.

This arrangement of counters and electronics reduced the beam contamination due to pions, muons and electrons to less than 0.3 % in the K^- beam, and to less than 0.05 % in the K^+ beam. Proton contamination in the K^+ beam is reduced to 0.2 % at 0.721 Gev/c, and decreases with the momentum. The principal rejection against protons

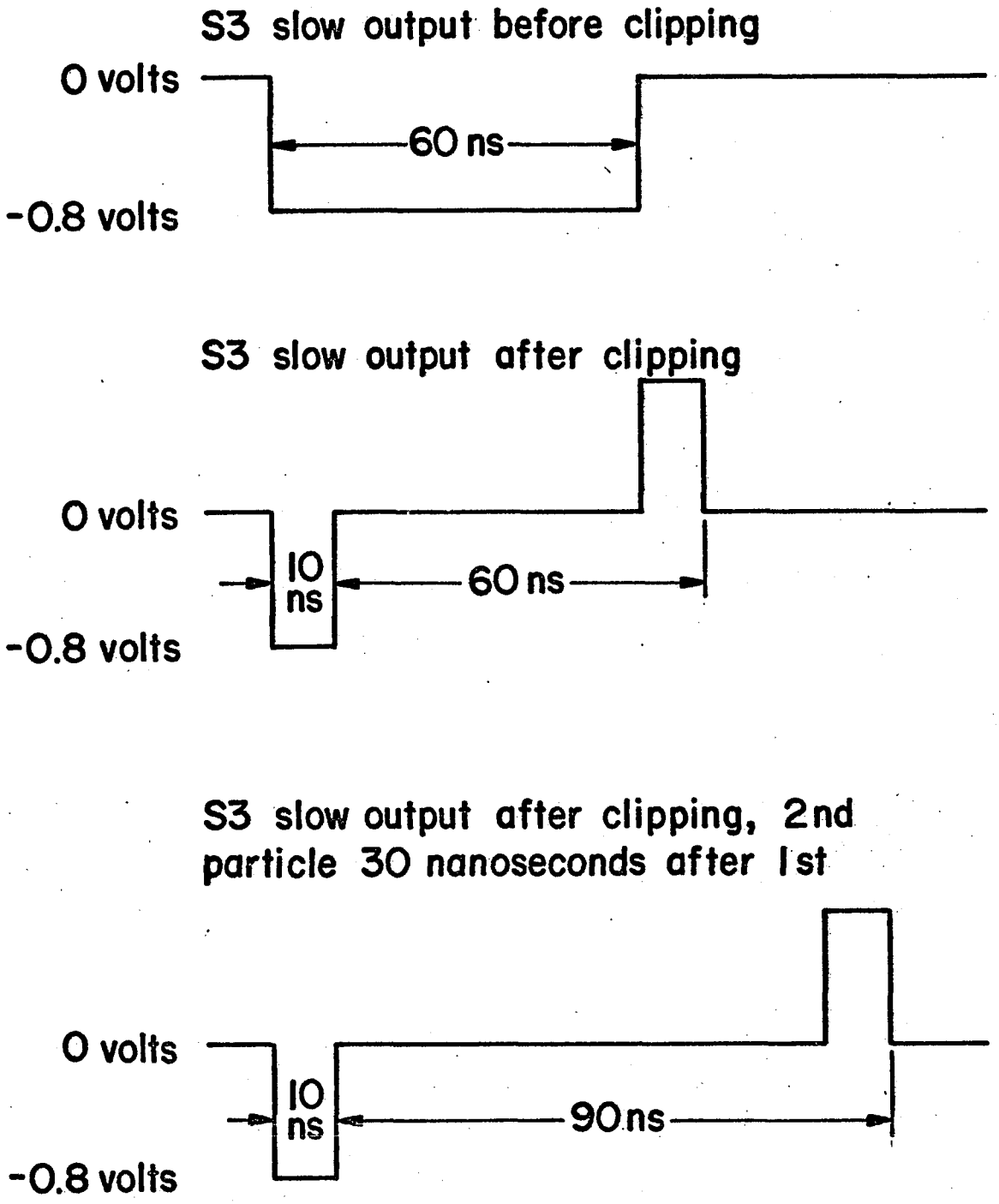

Figure 10. Elimination of accidentals by S3 slow.

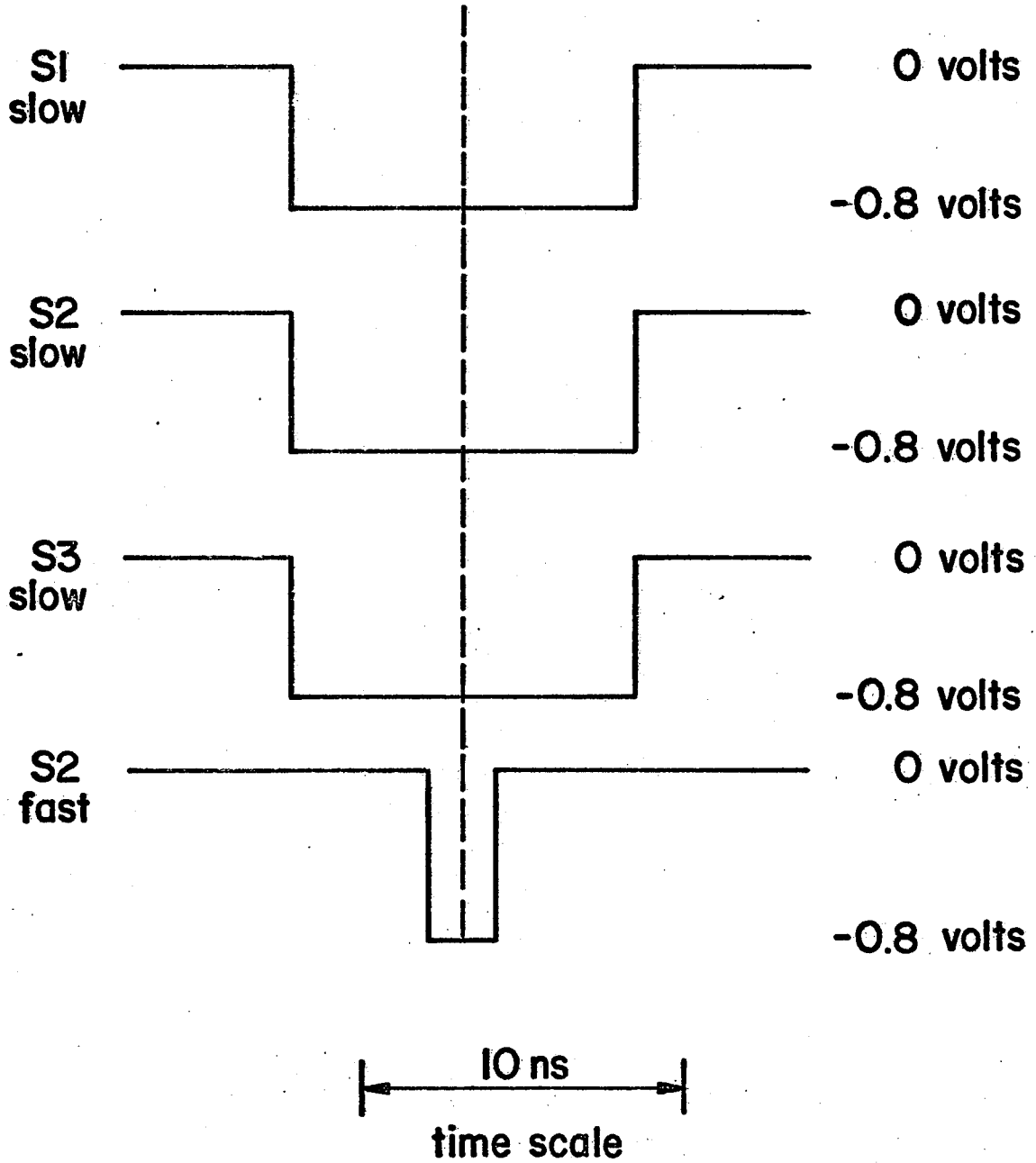

Figure 11. Inputs to $\overline{GS1S2S3}$.

is time-of-flight, with the dE/dx rejection providing an extra factor of 3 to 5, depending on the momentum.

Event Identification

Figure 12 shows the logic circuitry used to detect the forward-going protons. KS4S4 requires a signal in S4 slow large enough to specify an event proton, and a signal from S4 fast with a sufficient delay after the arrival of a kaon at S2 to rule out fast particles with a high degree of confidence. (KS4)S5$\overline{C2}$ includes the dE/dx information from S5 slow and the fast particle rejection of C2, and the output pulse is initiated by S5 fast.

This proton telescope rejected the non-interacting beam particles by a factor of 10,000 at the lower momenta, with a factor of 10 due to dE/dx measurements, and the rest due to the time-of-flight rejection by S4. At higher momenta these mechanisms became less effective, but C2 became operational, so that at 0.721 Gev/c a rejection factor of 1,000 against beam kaons was still possible.

When an event passed all of the logic requirements, S5 fast started the time-to-amplitude converter (TAC). The TAC was then stopped by the output of S2 fast, which had been appropriately delayed. The TAC information was then stored in a pulse height analyzer. The PHA was calibrated so that each channel was 1/4 nanosecond. The total resolution of the system was such that the peaks due to beam kaons or protons generated by turning off the appropriate rejection factor had widths at 1/2 the peak amplitude of 8 channels. The PHA was used to analyze

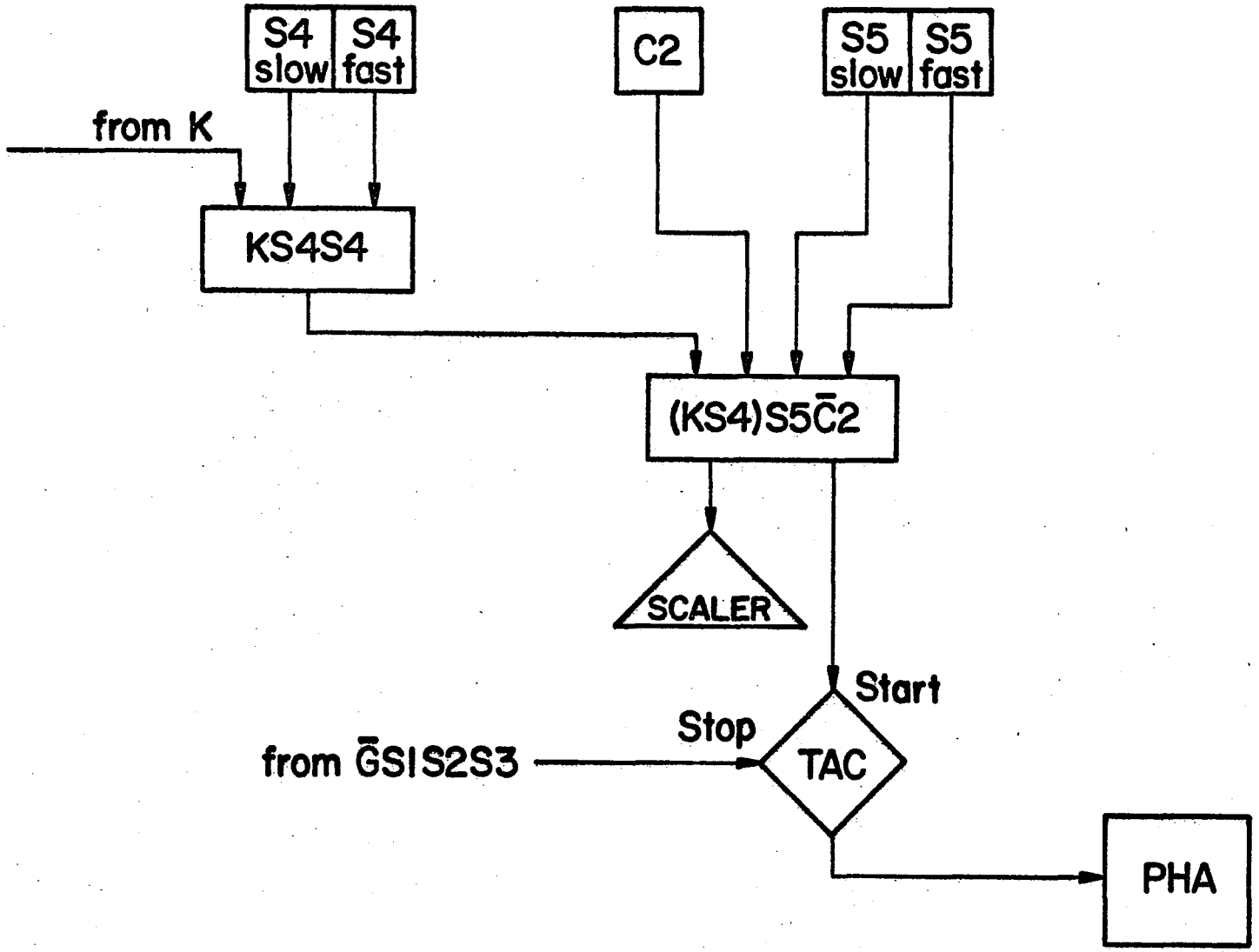

Figure 12. Proton telescope electronics.

all particles which passed the logic requirements and which had velocities less than that of a beam kaon, but were greater than 1/3 c.

The pulse height analyzer contents along with the scaler reading of the number of incoming kaons constituted the raw data.

DATA REDUCTION AND ANALYSIS

The raw data contained five possible kinds of contamination: 1) beam kaons not rejected by the proton telescope, 2) beam protons misidentified as incident K^+, 3) inelastic events in the case of K^-, such as $K^- p \rightarrow \Sigma^{\pm}\pi^{\mp}$, 4) background due to possible second particles accompanying a beam kaon, 5) $\pi^{\pm}$ p elastic scatters at 180°. In most cases the true events are a well-resolved peak in the S2-S5 time-of-flight spectrum, although the K^+ data at 0.721 Gev/c did require unfolding by a computer to distinguish the events from the K^+ and beam proton peaks on either side. The fitting was done by assuming all peaks to be gaussian with known centers, and adjusting the areas and widths to minimize the chi-square. An example of the pulse height analyzer contents is shown in Figure 13.

The peaks due to beam kaons and misidentified beam protons could always be positively identified by turning off an appropriate rejection mechanism and allowing data to accumulate in the PHA for a few minutes. These peaks were also seen in the empty target data, while peaks corresponding to events are seen only in the full target data.

Events due to $\pi^{\pm}$ p scatters were not distinguishable from $K^{\pm}$ p scatters. However, such contamination of the data was negligible, since the pion contamination of the beam was always less than 0.3 %, as discussed previously.

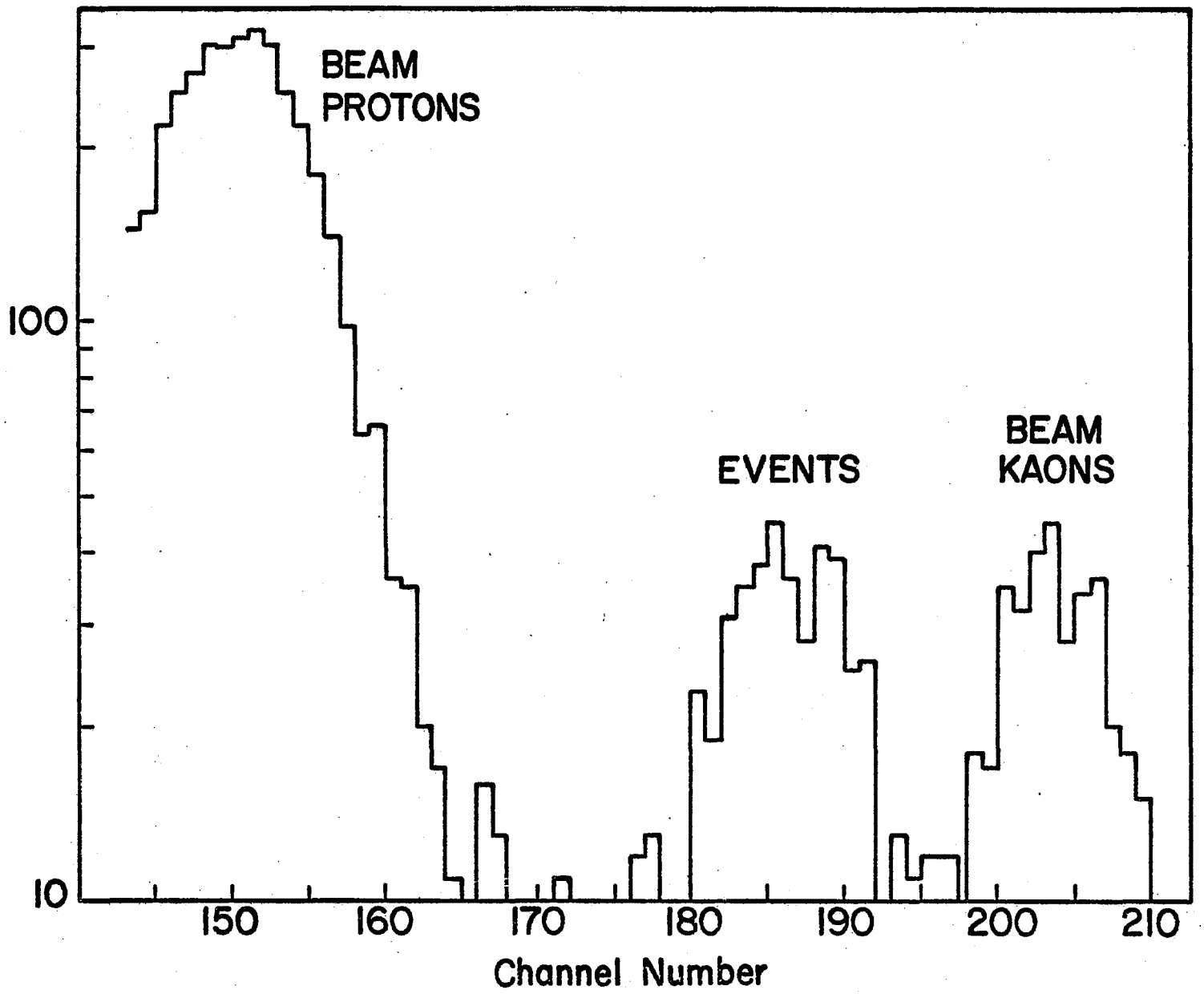

Figure 13. K+ full target data at 0.6 Gev/c.

Peaks due to inelastic events are not evident in any K^+ data. Any extraneous peaks in the K^- data, which might be identified as inelastic events, would not be as well-constrained kinematically as the elastic peak, and would be too broad to be confused with real events. The case of a beam particle accompanied by a second particle would also be expected to give a broad, flat background. A small amount of this was observed, but again the peak corresponding to events is always clearly distinguishable.

The number of events counted at each momentum is the number of events in the peak minus a background derived from the empty target data. In the case where a fit was done by computer, the empty target background was fitted, and the fitting parameters obtained there used in fitting the full target data. The number of events with statistical errors becomes,

$$N_{full} - \zeta N_{empty} \pm \sqrt{(N_{full} + \zeta^2 N_{empty})}$$

where N_{full} is the number of events observed in the full target running, N_{empty} is the background to be subtracted, and ζ is the ratio of incident beam on full target to incident beam on empty target.

Once the events were counted, the following corrections were made: a) decay and nuclear scattering of the kaon beam, b) nuclear scattering of the event protons, and c) multiple coulomb scattering of the protons in the target and in counters S4 and C2.

Correction a), the fraction F of kaons remaining after decays and scattering, is given by

$$F = e^{-X_1/L_o} \left\{ \frac{1}{X_2} \int_o^{X_2} e^{-X/L_o'} \, dx \right\}$$

$$= e^{-X_1/L_o} \left\{ \frac{L_o'}{X_2} \left(1 - e^{-X_2/L_o'} \right) \right\}$$

where the first factor on the right represents the decays between the last counter and the target, and the integral represents the average number of kaons in the target, considering losses due to decays and scatters. X_1 is the distance from the last Cherenkov counter to the target, X_2 is the target length, L_o is the mean decay length before the kaon reaches the target, and L_o' is a mean length which includes decays and nuclear scattering in the target. They are as follows:

$$L_o = (cp_1)\ (c\tau)/m_o c^2$$

$$L_o' = L_s L_d / (L_s + L_d)$$

$$L_s = w/\sigma A \rho$$

$$L_d = (cp_2)\ (c\tau)/m_o c^2 \ ,$$

where $m_o c^2$ is the rest mass of the kaon, .4938 Gev; $c\tau$ is its decay length, 370 cm.; w is the atomic weight of hydrogen, A is Avogadro's number, ρ is the density of hydrogen in the target, and σ is the appropriate $K^{\pm}$ p total cross-section. cp_1 is the incident momentum, and cp_2 is the beam momentum at the target's center, in Gev/c. Using the fixed momentum rather than cp as a function of position in the target may cause F to be in error by no more than .1 $^{o}/_{o}$.

The remaining corrections b) and c) were done on a computer using the Monte Carlo technique. Nuclear scatters of protons were distributed according to a mean scattering length L_p given by

$$L_p = w/A\rho\sigma$$

where the w's, ρ's, and σ's were the appropriate atomic weights, densities, and cross-sections of the counters and the target as traversed by the protons. Multiple coulomb scattering was described by the function (Rossi 1952, Sternheimer 1954)

$$P(\theta) = \frac{1}{\pi\theta_o^2} e^{-\theta^2/\theta_o^2} ,$$

where θ is the deviation from the incident trajectory, and

$$\theta_o = \frac{21 \text{ Mev}}{\beta cp}\left(\frac{L}{X_o}\right)^{\frac{1}{2}} .$$

p is the average momentum of the particle in the material, βc is the velocity, L the length of absorber traversed, and X_o the radiation length.

Having made these corrections, the differential cross-section at 180° may be calculated from the following equation.

$$\frac{d\sigma}{d\Omega} = \frac{N(\text{events})}{N(\text{kaons})} \times \left\{ \frac{w}{A\rho L} \right\} \times \frac{1}{\int_o^\pi \Phi(\theta) d(\cos\theta)}$$

where $N(\text{kaons}) = FN_o$, N_o being the number read by the beam telescope, w is the atomic weight of hydrogen, A is Avogadro's number, ρ is the

density of the liquid hydrogen target, and L is the target length.

$$\frac{W}{A\rho L} = 535 \text{ millibarns}$$

The integral represents the probability $\Phi(\theta)$ that a kaon scattered elastically at a center-of-mass angle θ will produce an event that will be detected. This integral may be replaced as follows

$$\int_0^{\pi} \Phi(\theta) d(\cos\theta) = E\,\Delta\Omega$$

where $\Delta\Omega$ is the solid angle subtended by the proton telescope, and E is the related counting efficiency of the system.

$E\Delta\Omega$ was also computed by the Monte Carlo technique. A computer generated events distributed evenly in the range $-.99 \geq \cos\theta_{c.m.} \geq -1.0$. These events were distributed in the target according to the measured beam distribution (Figure 8) and weighted with the same decay and scattering parameters used to determine F. It was found that only those events for which $\cos\theta_{c.m.} \leq -.995$ were observable, so that

$$\Delta\Omega = 2\pi(.005) \quad .$$

Then E is the total number of events counted by the computer divided by the total number of events generated for which $\cos\theta_{c.m.} \leq -.995$.

It is noteworthy that the Monte Carlo computer program used to calculate $E\Delta\Omega$ reproduces the measured number of beam protons scattered away from S5 by S4 and C2.

The quantity $E\Delta\Omega$, along with the values of $d\sigma/d\Omega$, are given in Tables II and III. The cross-sections are plotted in Figures 14 and 15, along with the results of previous experiments. The error bars represent the statistical uncertainty in the number of events, plus 1.33 % uncertainty contributed by the Monte Carlo analysis.

Table II

K^+ P DATA

P_{lab} (Gev/c)	N_{kaons}	F	N_{events}	$E\Delta\Omega$	$\frac{d\sigma}{d\Omega}\left(\frac{\text{millibarns}}{\text{steradian}}\right)$
0.407	0.993×10^7	.874	113 ± 14	.00734	0.92 ± .13
0.477	2.0×10^7	.889	234 ± 23	.00767	0.91 ± .11
0.539	2.0×10^7	.901	260 ± 21	.00791	0.90 ± .08
0.600	2.0×10^7	.909	315 ± 26	.00809	1.14 ± .11
0.660	1.5×10^7	.917	186 ± 30	.00835	0.85 ± .15
0.721	1.5×10^7	.923	194 ± 42	.00856	0.87 ± .19

Table III

K^- P DATA

P_{lab} (Gev/c)	N_{kaons}	F	N_{events}	$F\Delta\Omega$	$\frac{d\sigma}{d\Omega}\left(\frac{\text{millibarns}}{\text{steradian}}\right)$
0.407	1.2×10^6	.87	56 ± 11	.00734	3.87 ± .80
0.477	3×10^6	.89	64 ± 13	.00765	1.66 ± .35
0.539	3×10^6	.90	30 ± 7	.00791	0.75 ± .17
0.600	4×10^6	.91	11 ± 10	.00810	0.2 ± .2
0.660	4×10^6	.92	-4 ± 10	.00835	0.0 ± .2
0.721	4.3×10^6	.92	35 ± 17	.00856	0.54 ± .27

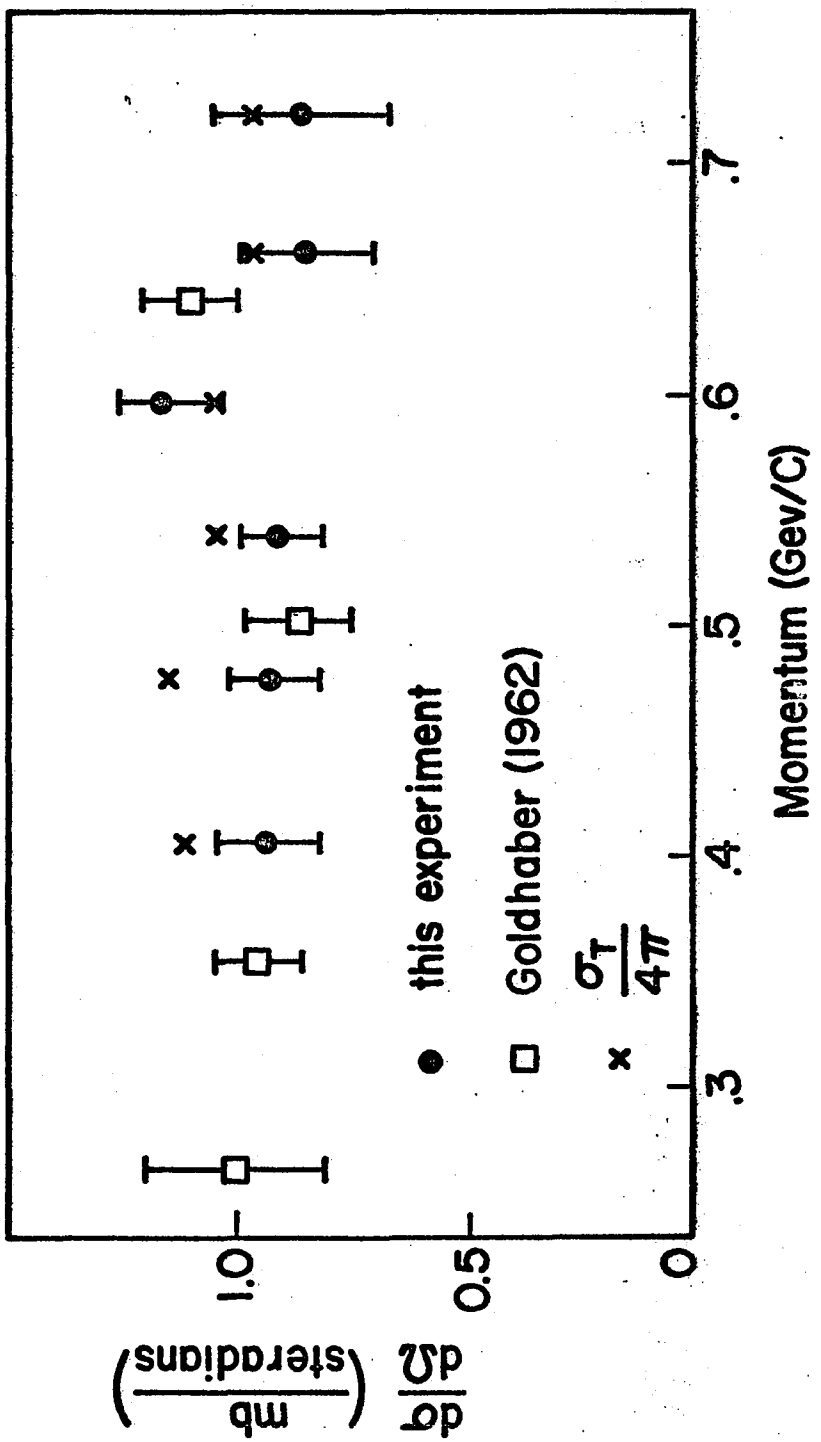

Figure 14. K^+ p cross-sections at 180°.

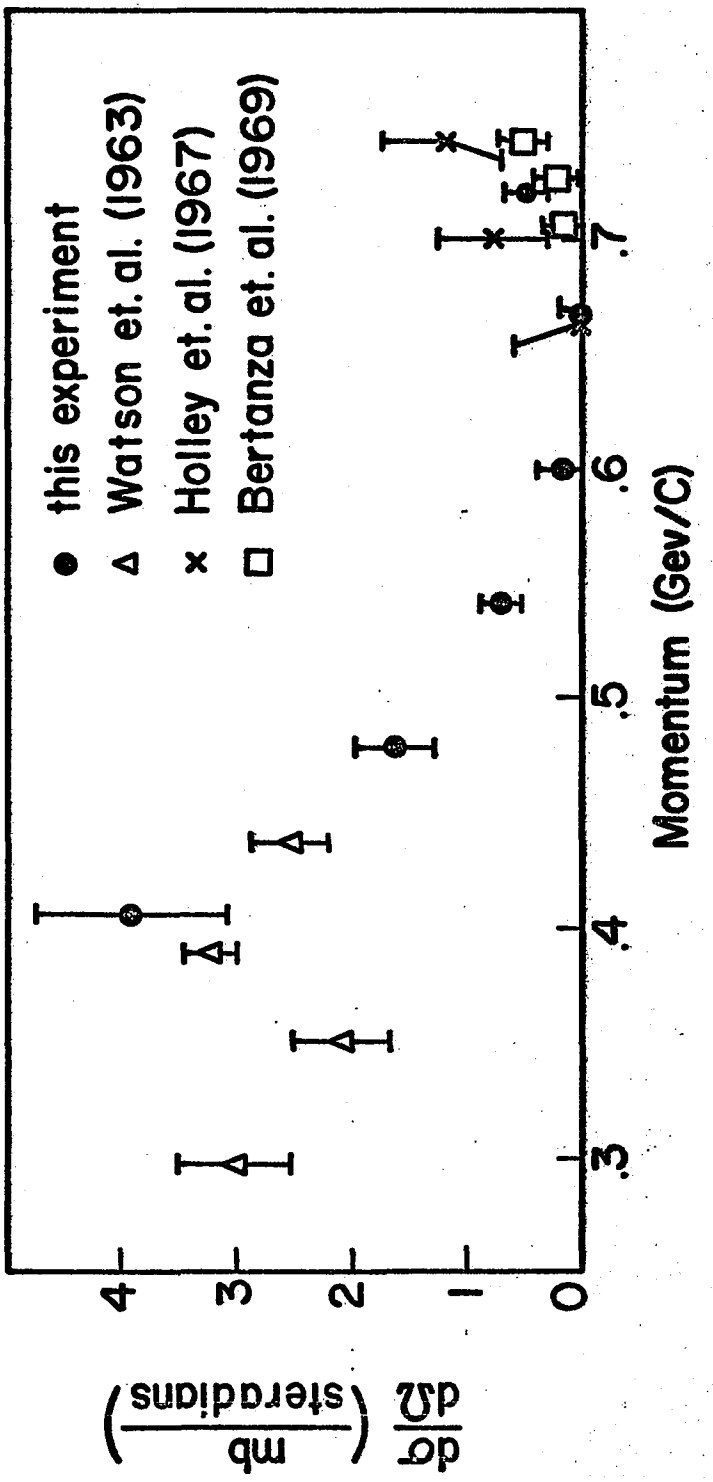

Figure 15. K^- p cross-sections at 180°.

DISCUSSION

The differential and total cross-sections of spin 0 particles striking a target of spin 1/2 particles can be expressed as (Kallen 1964)

$$\frac{d\sigma}{d\Omega} = |f(s,\theta)|^2 + |g(s,\theta)|^2 \tag{1}$$

$$\sigma_{total} = \frac{4\pi}{k} \sum_{\lambda=0}^{\infty} \left\{ (\lambda+1)\mathrm{Im}f_{\lambda+}(s) + \lambda \mathrm{Im}f_{\lambda-}(s) \right\} \tag{2}$$

Following the notation of Lea, Martin, and Oades (1968), the f's and g's are defined as

$$f_n(s,\theta) = \sum_{\lambda=0}^{\infty} \left\{ (\lambda+1)_{\lambda+}(s) + \lambda f_{\lambda-}(s) \right\} P_\lambda(\cos\theta)$$

$$f(s,\theta) = f_n(s,\theta) + f_c(s,\theta)$$

$$g(s,\theta) = \sum_{\lambda=0}^{\infty} \left\{ f_{\lambda+}(s) - f_{\lambda-}(s) \right\} P^1_\lambda(\cos\theta)$$

$$f_{\lambda\pm}(s) = \frac{\eta_{\lambda\pm}(s)\exp[2i\delta_{\lambda\pm}(s)]-1}{2ik}$$

In the foregoing equations, s is the square of the center of mass energy, θ the center of mass scattering angle, $P_\lambda(\cos\theta)$ and $P^1_\lambda(\cos\theta)$ are the Legendre polynomials and the associated Legendre polynomials, and k is the momentum in the center of mass system.

The $f_{\lambda\pm}$ represents the partial wave with angular momentum λ, $J = \lambda \pm 1/2$. The $\delta_{\lambda\pm}$ are the real phase shifts. $\eta_{\lambda\pm}$ is the elasticity, and represents directly the amplitude of the outgoing wave, hence $0 \leq \eta_{\lambda\pm} \leq 1$.

$f_n(s,\theta)$ denotes the part of $f(s,\theta)$ due to nuclear interaction only. The electromagnetic interaction is contained in the $f_c(s,\theta)$. The practice of adding f_c and f_n to obtain $f(s,\theta)$ is shown by Van Hove (1952) to introduce errors less than 1 $^0/_0$ in large angle scattering at high energies. Further, any of the several expressions for $f_c(s,\theta)$ (Roper, Wright, and Feld 1965) have a magnitude of only 1 $^0/_0$ or less that of $f_n(s,\theta)$ in $K^{\pm}$ p scattering at 180° above 0.4 Gev/c. Such a small correction is not within the resolution of this experiment.

At 180° these equations simplify. In particular

$$f(s,\pi) = \sum_{\lambda=0}^{\infty} \left\{ (\lambda+1)f_{\lambda+} + \lambda f_{\lambda-} \right\} (-1)^{\lambda} \quad ,$$

$$g(s,\pi) = 0 \quad .$$

To fit the K^+ p data to these equations, it is assumed that $\eta_{\lambda} \simeq 1$, so that

$$f_{\lambda\pm} \simeq \frac{1}{k} e^{i\delta_{\lambda\pm}} \sin\delta_{\lambda\pm} \quad . \tag{3}$$

Goldhaber et al (1962) points out that the inelastic cross-section for K^+ p is only about 0.5 $^0/_0$ of the total cross-section at 0.642 Gev/c, and about 8 $^0/_0$ at 0.810 Gev/c. Consequently, below 0.730 Gev/c, the η should not be less than .97. The phase shift analysis of Lea, Martin, and Oades (1968) supports this. Therefore, the parametrization of (3)

will be used. If one assumes that the K^+ p scattering is purely s-wave, then the total and differential cross-section should be related by

$$\frac{d\sigma}{d\Omega} = \sigma_t/4\pi \quad .$$

It can be seen from Table IV that this assumption does not fit the data.

If p- waves are also included, then

$$f_n(s,\pi) = \frac{1}{k}\left\{ e^{i\delta_{0+}} \sin\delta_{0+} - 2e^{i\delta_{1+}} \sin\delta_{1+} - e^{i\delta_{1-}} \sin\delta_{1-} \right\}$$

$$\sigma_t = \frac{4\pi}{k^2}\left\{ \sin^2\delta_{0+} + 2\sin^2\delta_{1+} + \sin^2\delta_{1-} \right\} \quad .$$

It is established by an examination of the interference of $f_c(s,\theta)$ and $f_n(s,\theta)$ at small angles that the s-wave phase shift δ_{0+} is negative (Goldhaber 1962). If it is assumed that the δ_1's are small (s-wave dominance) so that $e^{i\delta_{1\pm}} \simeq 1$, the quantity $(2\delta_{1+} + \delta_{1-})$ can be calculated. This is plotted as a function of momentum in Figure 16.

The analysis of the K^- p data is much more complex. Inelastic or exothermic processes may occur at all incoming beam momenta. Also, the momentum range of this experiment includes two known resonances, the $\Sigma(1610)$ and $\Sigma(1660)$, and goes very near to several others. Without the complete angular distributions it is not possible to discuss the phase shifts, since presumably more than s and p waves are always present.

The K^- elastic differential cross-section at 180° becomes very nearly zero (-4 ± 10 events) at 0.665 Gev/c. It has been suggested

Table IV

COMPARISON OF TOTAL CROSS-SECTION
WITH DIFFERENTIAL CROSS-SECTION

P	σ_t #	$\sigma_t/4\pi$	$d\sigma/d\Omega\|_{180°}$
.407 Gev/c	13.97 ± .26	1.11	.92 ± .13
.477 Gev/c	14.61 ± .47	1.17	.91 ± .11
.539 Gev/c	13.15 ± .36	1.05	.90 ± .08
.600 Gev/c	13.16 ± .18	1.05	1.14 ± .11
.660 Gev/c	12.35 ± .20	0.985	.85 ± .15
.721 Gev/c	12.37 ± .70	0.985	.87 ± .19

Data taken from an experiment by Bowen et al (to be published).

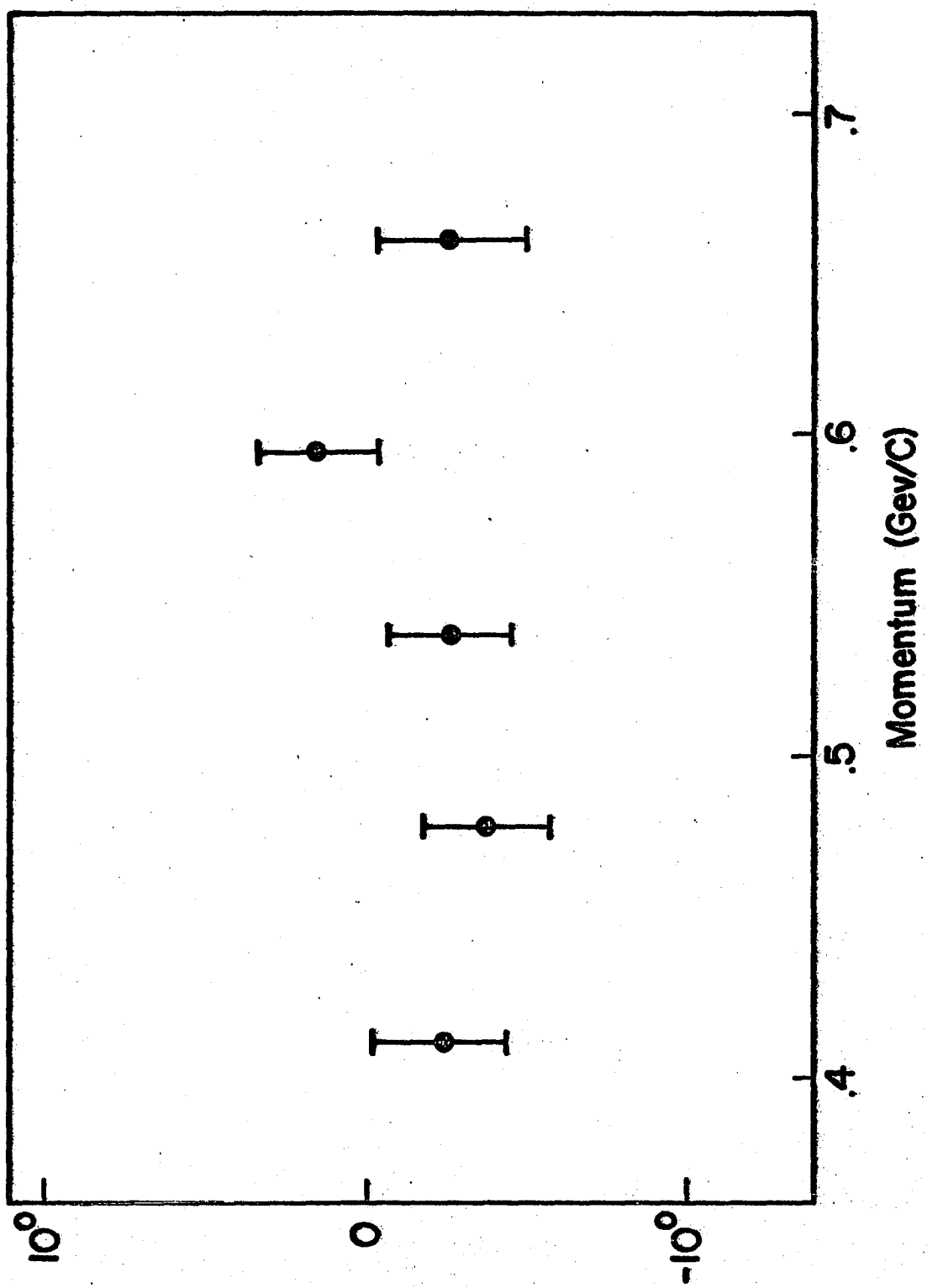

Figure 16. $2\delta_{1+} + \delta_{1-}$ between 0.4 and 0.7 Gev/c.

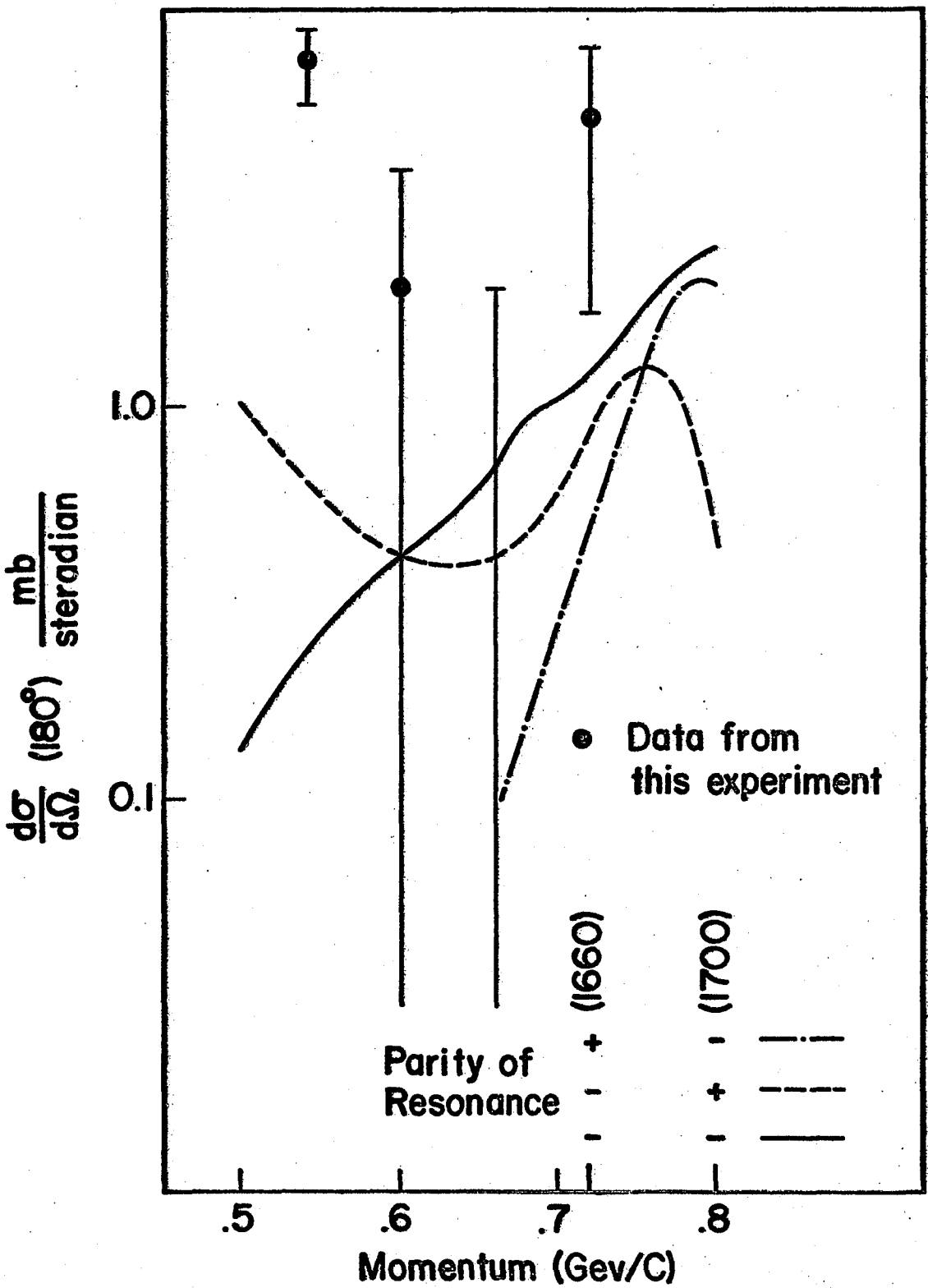

Figure 17. Comparison of the data with predictions based on the various parity assignments for the Λ(1660) and Λ(1700).

(Kormanyos 1966) that a resonant state of the opposite parity of the non-resonant background amplitude may cause such dips in the $d\sigma/d\Omega$ at 180°. However, the minimum does not lie on any known resonance. Another interpretation would be an interference between the amplitudes of the various Σ and Λ resonances. A recent prediction for the 180° elastic cross-section using the various possible parity assignments for the dominant resonances in the region 700-3000 Gev/c is shown in Figure 17 (Bertram et al 1967). The agreement with the data is poor in all cases.

Lastly, it is evident that the data do not conflict with existing $K^{\pm}$ p data near 180°. Clearly, there is no unexpected behavior of the $d\sigma/d\Omega$ in the extreme backward direction. The K^{+} data further precludes the existence of any resonant behavior in the K^{+} p system below 0.7 Gev/c.

LIST OF REFERENCES

Abrams, R. J., R. L. Cool, G. Giacomelli, T. F. Kycia, B. A. Leontic, K. K. Li, and D. N. Michael, Phys. Rev. Letters 19, 259 (1967).

Aderholz, M., J. Bartsch, E. Keppel, L. Rumpf, R. Speth, C. Grote, J. Klugow, H. W. Meier, D. Pose, M. Bardadin-Otwinowska, V. T. Cocconi, E. Flaminio, J. D. Hansen, H. Hromadnik, G. Kellner, M. Markytan, D. R. O. Morrison, D. P. Dallman, S. J. Goldsack, M. E. Mermikides, N. C. Mukherjee, W. W. Neale, A. Frohlich, G. Otter, I. Wacek, and H. Wahl, Phys. Lett. 24B, 434 (1967).

Banaigs, J., J. Berger, C. Bonnel, J. Duflo, L. Goldzahl, F. Plouin, W. F. Baker, P. J. Carlson, V. Chabaud, and A. Lundby, Phys. Lett. 24B, 317 (1967).

Barash-Schmidt, Naomi, Angela Barbaro-Galtieri, Leroy R. Price, Arthur H. Rosenfeld, Paul Soding, Charles G. Wohl, Matts Roos, and Gianni Conforto, Rev. Mod. Phys. 41, 109 (1969).

Bertanza, L., A. Bigi, R. Carrara, R. Casali, R. Pazzi, D. Berley, E. L. Hart, D. C. Rahm, W. J. Willis, S. S. Yamamoto, and N. S. Wong, Phys. Rev. 177, 2036 (1969).

Bertram, W., L. Holloway, L. Koester, R. Thatcher, A. Wattenberg, University of Illinois proposal P-187 at the ZGS.

Bevatron Experimenter's Handbook, UCRL Report 17333, 1969 (unpublished).

Bowen, Theodore, Paul Caldwell, F. Ned Dikmen, Edgar W. Jenkins, Robert M. Kalbach, Douglas V. Petersen, and Alburt E. Pifer, (to be published).

Carroll, A. S., J. Fischer, A. Lundby, R. H. Phillips, C. L. Wang, F. Lobkowicz, A. C. Melissinos, Y. Nagashima, C. A. Smith, and S. Tewksbury, Phys. Rev. Letters 21, 1282 (1968).

Derrick, M., CERN Report 68-7, Vol. I, Topical Conference on High-Energy Collisions of Hadrons, 1968 (unpublished).

Ficenec, J. R. and W. P. Trower, Phys. Lett. 25B, 369 (1967).

Goldhaber, Sulamith, William Chinowsky, Gerson Goldhaber, Wonyong Lee, Thomas O'Halloran, Theodore F. Stubbs, G. M. Pjerrou, Donald H. Stork and Harold K. Ticho, Phys. Rev. Letters 9, 135 (1962).

Heinz, Richard M., and Marc H. Ross, Phys. Rev. Letters 14, 1091 (1965).

Holley, W. R., E. F. Beall, D. Keefe, L. T. Kerth, J. J. Thresher, C. L. Wang, and W. A. Wenzel, Phys. Rev. 154, 1273 (1967).

Kallen, Gunnar, Elementary Particle Physics. Reading: Addison-Wesley, 1964.

Kormanyos, S. W., A. D. Krisch, J. R. O'Fallon, K. Ruddick, and L. G. Ratner, Phys. Rev. Letters 16, 709 (1966).

Kycia, T. F., L. T. Kerth, and R. G. Baender, Phys. Rev. 118, 553 (1960).

Lea, A. T., B. R. Martin, and G. C. Oades, Phys. Rev. 165, 1770 (1968).

Roper, L. David, Robert M. Wright, and Bernard T. Feld, Phys. Rev. 138, B190 (1965).

Rossi, Bruno. High Energy Particles. Englewood Cliffs: Prentice Hall, Inc., 1952.

Sternheimer, R. M., The Review of Scientific Instruments 25, 1070 (1954).

Stubbs, Theodore F., Hugh Bradner, William Chinowsky, Gerson Goldhaber, Sulamith Goldhaber, William Slater, Donald M. Stork, and Harold K. Ticho, Phys. Rev. Letters 7, 188 (1961).

Van Hove, Leon, Physical Review 88, 1358 (1952).

Watson, Mason B., Massimiliano Ferro-Luzzi, Robert D. Tripp, Phys. Rev. 131, 2248 (1963).